COMPARISON OF STORY DRIFT DEMANDS OF VARIOUS CONTROL STRATEGIES FOR THE SEISMIC RESISTANCE OF STEEL MOMENT FRAMES

Luciana R BARROSO[1], Scott E BRENEMAN[2] And H. A SMITH[3]

SUMMARY

The research presented here evaluates different structural control methods by comparing their impact on overall structural performance, under seismic excitations. This study focuses on steel moment resisting frames and several types of possible controllers: 1) friction pendulum base isolation system, 2) linear viscous dampers, and 3) active tendon brace system. These control approaches are applied to the three story steel moment resisting frame structure located in the Los Angeles region that was developed for the SAC Phase II project. Simulations of these systems, both controlled and uncontrolled, are prepared using the three suites of earthquake records, also from the SAC Phase II project, that represent three different expected return periods. The system performance is judged based on interstory drift demands determined through nonlinear dynamic analyses. Simulation results indicate that structural control system are effective solutions that can improve structural performance, though no one system is best over all different excitation levels. All three control strategies investigated can significantly reduce the seismic drift demands on a structure, thereby reducing the expected damage to the structure.

INTRODUCTION

The structural engineering community has been making great strides in recent years to develop performance-based earthquake engineering methodologies for both new and existing construction. New provisions, such as the *NEHRP Guidelines for Seismic Rehabilitation of Buildings* [BSSC, 1997], present the first set of guidelines for multi-level performance objectives in the United States. One of the intents of these provisions is to provide methods for designing and evaluating structures such that they are capable of providing predictable performance during an earthquake.

For structural control to gain viability in the earthquake engineering community, understanding the role of controllers within the context of performance-based engineering is of primary importance. Design of a structure/controller system should involve a thorough understanding of how various types of controllers enhance structural performance, such that the most effective type of controller is selected for the given structure and seismic hazard. Controllers may be passive, requiring no external energy source, or active, requiring an external power source. Applications of certain passive systems, including base isolation and viscous dampers, have become more common, leading to a reasonable understanding of how such systems reduce the dynamic behaviour of structures. However, few full-scale applications of active controllers exist and their enhancement of structural performance, particularly for larger events, is less understood.

The objective of the research presented here is to evaluate different structural control strategies based on their impact on the overall structural performance under seismic excitations. This study focuses on steel moment resisting frames, and various types of possible controllers, including both active and passive systems. A three story steel moment-resisting frame structure located in the Los Angeles region is selected from the SAC Phase II project. Simulations of these systems, both controlled and uncontrolled, are prepared using the three suites of earthquake records, also from the SAC Phase II project, representing three return different periods. Several controllers are developed for the structure, and the system's performance is judged based on the interstory drift demands.

[1]   Dept. of Civil Engineering, Texas A&M University, College Station TX, 77843-3126; lbarroso@civilmail.tamu.edu
[2]   Dept. of Civil and Environmental Engineering, Stanford University, Stanford CA, 94305-4020; breneman@stanford.edu
[3]   Dept. of Civil and Environmental Engineering, Stanford University, Stanford CA, 94305-4020; smith@gofannon.stanford.edu

PERFORMANCE EVALUATION

One of the first requirements of performance evaluation is the selection of one or more performance objectives, i.e.: select desired performance level and associated seismic hazard level. Since the evaluation relies on analysis rather than experimentation, the criteria should be stated in terms of a response that can be calculated. Depending on the intensity of the ground motion, a different performance objective will be desired. According to the expected intensity, the designer must analyse whether achieving the desired objective will be economically feasible. For frequent events, the designer will probably desire that the structure remain fully operational. For rarer events, ensuring prevention against collapse may be the only realistic goal.

Performance may be concerned with structural and nonstructural systems as well as contents, and behaviour ranging from minor damage to failure. In general, different performance levels will require different design criteria to be applied to different design parameters. At one end of the performance spectrum, content damage is often proportional to floor accelerations, which can be limited by reducing stiffness. At the other end of the spectrum, life safety and collapse prevention are controlled by inelastic deformation capacity of ductile members and strength capacity of brittle members. As a result, no single design parameter may satisfy all performance requirements.

No single damage measure will provide all the information required to assess structural performance, especially at all performance objectives. However, some indicator must be used to provide quantitative limits. Peak transient drift serves as an indicator of damage to low strength rigid elements, such as building cladding and partition walls, and the maximum deformation of the structural elements. The use of maximum values as an indicator of damage provides preliminary information to be used in the evaluation of the structural system

PROBLEM DEFINITION

This investigation has the specific objective of evaluating the effect of the various controller architectures on seismic demands as described through performance-based design criteria. We believe it is critical, in the practical evaluation of the performance of buildings---whether controlled or not---under seismic threats to reflect (1) the realistic potential for nonlinear behaviour and (2) the realistic characteristics of ground motion excitations (i.e., by imposing a suite of recorded ground motion records, as opposed to an idealised probabilistic, random vibration description).

Structure

The structure analyzed is a three-story steel moment-resisting frame buildings (SMRF) designed as part of the SAC steel project for the Los Angeles area. These buildings conform to local code requirements. The structure is an office building designed for gravity, wind, and seismic loads, with a basic live load of 2.4 kPa (50 psf). The structural system for all buildings consists of steel perimeter moment frames and interior gravity frames with shear connections. All columns in the perimeter frame that are part of the lateral force-resisting system bend about the strong axis. The North-South frame of the 3-story structure has three fully moment resisting bays and one simply-connected bay, as shown in Figure 1. The columns are fixed at the base and run the full height of the structure. The dimensions shown in Figure 1 are centreline dimensions, and the section sizes are listed next to each corresponding member.

The structures are modelled as two-dimensional frames that represent half of the structure in the north-south direction. The frame is given half of the seismic mass of the structure at each floor level. A basic centerline model of the bare moment resisting frame is developed for both structures. The strength, stiffness, and shear distortions of panel zones is neglected. A finite element model of the structure was developed where an assembly of interconnected elements describes the hysteretic behaviour of structural members. The inelastic behaviour of the members is taken to be concentrated at the end of girders and beams. Thus each structural member is constructed using a lumped plasticity model with nonlinear rotational springs at each end joined by a linear beam-column element.
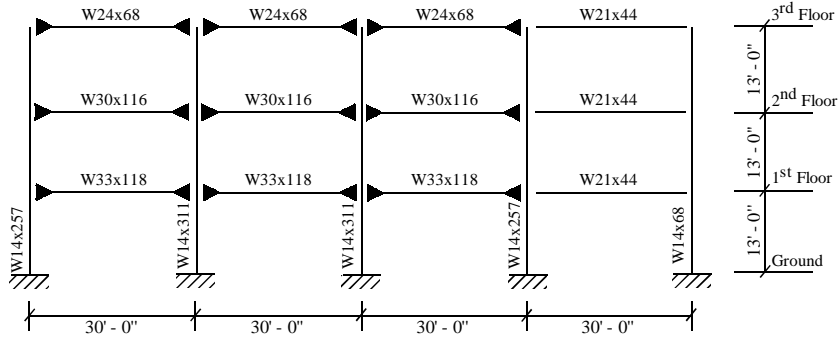
Figure 1: 3-Story Moment-Resisting Frame

Hysteresis Modelling

The Bouc-Wen [Wen, 1976] smooth-varying hysteretic model is utilised for the nonlinear rotational spring. This model includes a number of parameters, allowing a mathematically tractable state-space representation capable of expressing several hysteretic properties.

The restoring force, f_R, for a single nonlinear element i may be decomposed into two parts, f_E and f_H, representing the elastic and hysteretic components respectively. The restoring force can then be written as:

$$f_R = f_E + f_H = k_e r(t) + k_h z(t) = \alpha\, k_T (r_a - r_b) + (1 - \alpha)\, k_T z(t) \tag{1}$$

where α is the ratio of the post-yielding to pre-yielding stiffness and k_T is the pre-yielding stiffness. The variable $r(t)$ is the relative deformation, r_a and r_b are the absolute displacements at nodes a and b respectively, and $z(t)$ is the corresponding variable introduced to describe the hysteretic component. The elastic component is used to represent the strain-hardening in the element. The force-deformation curve is described by:

$$\dot{z} = \dot{r}\left[1 - 0.5\left(1 + \mathrm{sgn}(\dot{r}z)\right)\left|\frac{z}{Y}\right|^n \right] \tag{2}$$

where Y is yield displacement and n is a shaping parameters [Wen, 1976; Barroso, 1999].

The resulting hysteretic behaviour described above is a stable force-deformation curve. The use of constant strain-hardening with the stable hysteretic loop ignores the presence of cyclic hardening and does not permit modelling of deterioration due to local instabilities. These effects could be captured through modification of the above equations.

Now consider a structure idealised by an n degree-of-freedom system under a one-dimensional earthquake ground motion. The equation of motion for the system can be expressed as:

$$\mathbf{M}\ddot{\mathbf{x}}(t) + \mathbf{C}\dot{\mathbf{x}}(t) + \mathbf{K_E}\mathbf{x}(t) + \mathbf{K_H}\mathbf{x}(t) = \mathbf{F_g}(t) \tag{3}$$

in which $\mathbf{x}(t)$ is a vector containing the displacement of each degree of freedom relative to the ground, and $\mathbf{z}(t)$ is a vector containing the corresponding hysteretic information for each element. $\mathbf{M}$ is the mass matrix and $\mathbf{C}$ is the viscous damping matrix. The ground motion, $\mathbf{F_g}$, is found by mapping the horizontal ground acceleration to the horizontal degrees of freedom through the vector and multiplying by $\mathbf{M}$. As in the single element case, the elastic and hysteretic components of the structural restoring force can be separated so that the restoring force is a function of both $\mathbf{x}(t)$ and $\mathbf{z}(t)$. The equation of motion for the system can be written in a nonlinear state-space format as:

$$\left\{\begin{array}{c} \dot{\mathbf{x}}(t) \\ \ddot{\mathbf{x}}(t) \\ \dot{\mathbf{z}}(t) \end{array}\right\} = \left[\begin{array}{ccc} \mathbf{0} & \mathbf{I} & \mathbf{0} \\ -\mathbf{M}^{-1}\mathbf{K_E} & -\mathbf{M}^{-1}\mathbf{C} & -\mathbf{M}^{-1}\mathbf{K_H} \\ \mathbf{0} & \left[{d\mathbf{z}}/{d\mathbf{x}}\right] & \mathbf{0} \end{array}\right] \left\{\begin{array}{c} \mathbf{x}(t) \\ \dot{\mathbf{x}}(t) \\ \mathbf{z}(t) \end{array}\right\} + \left[\begin{array}{c} \mathbf{0} \\ \mathbf{M}^{-1} \\ \mathbf{0} \end{array}\right]\mathbf{F_g}(t) \tag{4}$$

where $\left[{d\mathbf{z}}/{d\mathbf{x}}\right]$ is a non-square matrix function found by mapping the individual contributions, from Equation (2), to the global co-ordinate system [Barroso et al., 1998].

Earthquakes

Suites of ten time histories were generated by Paul Somerville [Somerville, 1997] to represent ground motions having probabilities of exceedance of 50% in 50 years, 10% in 50 years, and 10% in 250 years in the Los Angeles region. These sets of ground motions are referred to as the 50 in 50 Set, 10 in 50 Set, and 2 in 50 Set respectively throughout this study. The time histories have magnitude-distance pairs that are compatible with the deaggregation of the probabilistic seismic hazard. Individual time histories were scaled so that their response spectra are compatible with the spectral ordinates from the 1996 USGS probabilistic ground motion maps, adjusted for site conditions from soft rock to stiff soil (from SB/SC boundary to SD), in the period range of 0.3 to 4 seconds. A single scaling factor was found for each time history that minimised the squared error between the target spectrum and the average response spectrum of the two horizontal components of the time history assuming lognormal distribution of amplitudes. The weights used were 0.1, 0.3, 0.3, and 0.3 for periods of 0.3, 1, 2, and 4 seconds respectively. The scale factor was then applied to all components of the time history.

An important note regarding the earthquake sets is that they should be used only as a set, and not individually or as small sub-sets as representative of the probability levels specified. At any particular period the median spectral acceleration of the set may match the target value reasonably well; however, any individual record may have a value quite different than the expected target spectral acceleration.

CONTROL SYSTEMS

Three basic types of control systems are used: (1) isolation systems, (2) passive damper systems, and (3) active control systems. A representative control system was chosen from each type listed above for implementation. These systems are: (1) the friction pendulum isolation system, (2) the linear fluid viscous damper system, and (3) the active tendon brace system. The basic design and implementation of these systems is described in the following subsections. More detailed information on the selection and design of these systems can be found in Barroso [1999] and Breneman [1999].

Friction Pendulum System (FPS)

The friction pendulum bearing (FPS) consists of an articulated slider on a spherical surface, which is faced with a polished stainless-steel overlay. The force needed to produce a displacement in the bearing consists of a restoring force, due to the rising of the structure along the spherical surface, and a frictional force along the sliding interface. The relationship between the isolation period and the radius of curvature, R, is:

$$R = g\left(\frac{T}{2\pi}\right)^2 \tag{5}$$

The horizontal force-displacement relationship that develops at the sliding interface is described by:

$$F_f = \frac{W^*}{R}u_f + \mu_S W^* z_f = k_{e,f}\,u_f + k_{h,f}\,z_f \tag{6}$$

where W^* is the effective weight carried by the bearing, μ_S is the friction coefficient, and z_f is a dimensionless variable bounded by ± 1, based on the Bouc-Wen model described previously. The frictional properties of PTFE (teflon) and stainless steel are characterised by [Constantinou, 1991]:

$$\mu_S = f_{\max} - \left(f_{\max} - f_{\min}\right)\exp(-a|\dot{u}|) \tag{7}$$

where $\dot{u}$ is the velocity of sliding, f_{max} is the coefficient of sliding friction at high velocity, f_{min} is the coefficient of sliding friction at low velocity, and a is a coefficient controlling the dependency of friction on sliding velocity. Similarly to the nonlinear spring element, the FPS element also places an entry into $\left[\frac{dz}{d\mathbf{x}} \right]$ in Equation (4).

Isolation systems with varying isolation periods, frictional surfaces, and number of bearings were investigated to determine the impact of these parameters on structural demands for this structure [Barroso, 1999]. The isolation system selected has a 3 second isolation period and a teflon-steel sliding interface with frictional properties: $f_{max} = 11.93\%$, $f_{min} = 2.66\%$, and $a = 0.6$.

Linear Viscous Damper System

Viscous dampers (VS), such as fluid cylinders, can be designed to provide a purely viscous force to the surrounding structure. The VS dampers studied are assumed to be linear in nature. The brace support for the damper is assumed to be rigid compared to the damper, so that all deformation in the system occurs through damper deformation. The dampers are located in the centre of the moment resisting frame and are arranged so that one damper runs diagonally across each story. Damping systems are designed through the selection of the damping constant, C_d, for each damper. The constitutional force-deformation relationship for the damper system, including both stiffness and damping terms in matrix format, can be expressed as follows:

$$\begin{Bmatrix} F_{d,i} \\ F_{d,j} \end{Bmatrix} = C_d \begin{bmatrix} 1 & -1 \\ -1 & 1 \end{bmatrix} \begin{Bmatrix} \dot{u}_{d,i} \\ \dot{u}_{d,j} \end{Bmatrix} + K_d \begin{bmatrix} 1 & -1 \\ -1 & 1 \end{bmatrix} \begin{Bmatrix} u_{d,i} \\ u_{d,j} \end{Bmatrix} \tag{8}$$

where $u_{d,i}$ and $u_{d,j}$ are the displacements at the i and j end of the damper respectively. The above equations are similar to those for linear truss elements, except that it contains both velocity and displacement terms in the local coordinate system. After transformation to the global coordinate system, the matrix corresponding to the displacement proportional terms are assembled into the global elastic stiffness matrix while the matrix corresponding to the velocity proportional terms are assembled into the global damping matrix in Equation (4).

The systems investigated have critical damping ranging from 10% to 40% of critical for the fundamental modes of vibration, as determined through the modified modal strain energy method [Fu, 1998]. In addition, different distributions over the height of the structure, resulting in the same total effective damping, were investigated. The system selected for comparison has equal size dampers on all three stories of the structure and provides 30% effective damping in the first mode of the structure.

Active Brace System

An active tendon system was chosen for implementation in the structure. This particular actuator system was chosen because its force application is similar to that of a passive viscous brace system, allowing for a more direct comparison between the two systems. Specifications for active vibration controller include those for the control algorithm and the control architecture, which includes the actuator and sensor specifications. The actuators are located in the centre of the moment-resisting frame and are arranged so that one actuator runs diagonally across each story. The actuators all have a saturation level of 1000kips. Accelerometers are utilised as sensors and are placed to measure horizontal oor accelerations at all floors above ground level. A robust H_∞ controller was developed for the above architecture using interstory drifts as the regulator response quantity.

The design model represents the real system to the controller design optimisation procedures, thus should be a realistic as needed to characterise the behaviour of the physical system that impact the effectiveness of the controller.

During the controller design, the structural dynamics of all of the structural systems used in this research are modeled as linear dynamic systems. The control design utilised here augments the nominal dynamic system with additional frequency weighted uncertainties. Ground motion excitation is modeled as an unknown external excitation with characteristic frequency content modeled using Kanai-Tajimi filters. Sensors are assumed to be unbiased and each sensor has some small level of independent white noise error that is modeled as an external excitation. Actuators in the design model are assumed to be band-limited in capacity and have errors represented by an independent white noise excitation added to the command signal of each actuator. During the design of the control system, calculations were performed on a reduced-order, nominal model of the structure. Traditional

structural dynamic reduction techniques such as modal truncation or Guyan reduction are applied. The application of the Guyan reduction is performed on the state-space form of so that the actuator and sensor mapping matrices are transformed as well as the basic structural dynamics. Also, the degrees-of-freedom (and states) of the reduced system are in terms of inter-story drift values, not floor displacements relative to the ground. Designing active controllers for this structure is discussed in detail in Breneman [1999].

Specific elements are available to represent the actuators and sensors in the active control system. Both require information regarding the noise bandwidth and saturation level for the actuator element. The controller algorithms integrated with the above analytical model are linear dynamic output feedback controllers of the form:

$$\dot{\mathbf{x}}_c(t) = \mathbf{A}_c \mathbf{x}_c(t) + \mathbf{B}_c \mathbf{y}(t)$$
$$\mathbf{w}(t) = \mathbf{C}_c \mathbf{x}_c(t) + \mathbf{D}_c \mathbf{y}(t)$$

$$(9)$$

where $\dot{\mathbf{x}}_c(t)$ is the state vector of the dynamic controller, $\mathbf{y}(t)$ is the sensor reading vector, $\mathbf{w}(t)$ is the controller command signal, and the constant matrices $\mathbf{A}_c$, $\mathbf{B}_c$, $\mathbf{C}_c$ and $\mathbf{D}_c$ are the linear state description of the regulator. The controller command signal $\mathbf{w}(t)$ is mapped to forces applied to the structure by the equation:

$$\mathbf{F}_u(t) = \mathbf{B}_u \mathbf{w}(t)$$

$$(10)$$

which is an additional force input to the state equations with the same mapping as $\mathbf{F_g}$ in Equation (5). The sensor measurements are described by mapping the states to the absolute accelerations at the sensor locations as:

$$\mathbf{y}(t) = \mathbf{C}_y(-\mathbf{M}^{-1}\mathbf{C}\mathbf{x}(t) - \mathbf{M}^{-1}\mathbf{K}_E\mathbf{x}(t) - \mathbf{M}^{-1}\mathbf{K}_H\mathbf{z}(t) + \mathbf{F}_u(t))$$

$$(11)$$

where $\mathbf{C}_y$ selects which accelerations are available. Equation (13) is combined with the open-loop structure state-space equation given in Equation (5) to form the controlled system with the augmented state vector, $\dot{\mathbf{x}}_s(t)$. The controller loop from the sensors to the actuators is algebraically closed to form the followin state-space equation.

$$\dot{\mathbf{x}}_s(t) = \mathbf{A}(\mathbf{x}_s(t)) \, \mathbf{x}_s(t) + \mathbf{B}_w \mathbf{F}_g$$

$$(12)$$

EVALUATION OF DRIFT DEMANDS

A wide consensus exists in the earthquake engineering community that for moment-resisting frames the interstory drift demand, expressed in terms of the interstory drift angle, is the best indicator of expected damage. As a global parameter, interstory drift is much more appropriate than the roof drift angle because in individual stories it may exceed the latter by a factor of two or more [Krawinkler and Gupta, 1998]. The use of story substructures permits also the estimation of element force and deformation demands from the story drift angle. As a representative value, the median (exponent of the average value of the log of the data) is selected, while the 84th percentile, assuming a lognormal distribution, is utilized to provide an indication of the scatter of the results. The values suggested for peak story drift angles in FEMA 273 can be used as one set of guidelines by which performance of a SMRF structure may be judged.

In the 50 in 50 set of ground motions, shown in Figure 2, the median values of drift demands remain fairly constant over the height of the structure. In all three controlled systems, the drift angles are below the estimated yield point of 1%. The largest drift ratio occurs at the top story except for the viscous system, where the largest drift ratio occurs in the second story. These same trends can be observed for the median values of the 10 in 50 set of ground motions, shown in Figure 3. All three controllers reduce the drift demands below the 2.5% life-safety limit. However, the relative placement of the demand curves for each system changes. In both cases, all three control strategies reduce the story drift demands over the entire height of the structure. In the50 in 50 set of ground motions, the viscous control system results in the lowest drift demands. Under the stronger ground motions of the 10 in 50 set, the FPS isolation system becomes more effective at reducing story drift demands. The isolation system only starts to become effective once the base shear reaches the sliding force of the bearing. Consequently, this system is not as effective at low level ground motions. The ATB system has comparable drift

demands with the passive system. The differences between systems becomes more pronounced at the 84th percentile values, though the same trends occur.

Under the 2 in 50 set of ground motions, significant nonlinearities occur in the controlled systems. Furthermore, the differences between control systems become more pronounced, as seem in Figure 4. While the FPS isolation system results in the lowest median drift demands, the effect of higher scatter can be seen when comparing the median and the 84th percentile values. In comparison, the results for the viscous system display less scatter. The ATB system has drift demands that are higher than both passive systems, though significantly reduced from the uncontrolled case. Again, the 84th percentile values indicate drift demands that increase more than those for the viscous system. However, for all controlled systems the median values are well below the collapse prevention limit of 5%. Since the placement of the actuators and their saturation level were designed to provide a comparable system between the ATB and VS controller, the only difference lies in the control strategy and not the physical limitations of the systems.

Care must be taken not to assume that control strategies that reduce statistical values for the ground motion sets will reduce demands for all individual excitations. In a motion-by-motion comparison, occasionally both active and passive control system do make performance worse [Barroso, 1999]. For this structure and sets of ground motions, the FPS isolation system always reduced roof and story drift angles. The same is not true for the VS and ATB system. In the VS controlled system, three ground motions within the 2 in 50 set led to slightly higher drifts in the first story. Similarly, two ground motions in the 2 in 50 set increase peak drift angles for both first and second stories with the ATB control system.

CONCLUSIONS

For short return periods, the addition of structural control reduced the median story drift by nearly 50%. However, the most significant impact of control occurs with the 2 in 50 ground motions. The uncontrolled structure has a median response just under the collapse prevention limit. The ATB and VS control systems bring the median response to about 3%, with the VS system resulting in less scatter in the data. The FPS isolation has the lowest median response, with values of about 1.5%. An important observation is that no one systems is best over all three excitation levels. Selection of a control strategy depends on the goals of the engineer.

Care must be taken in the interpretation of the above results. While peak interstory drift provides a good indication of performance, the resulting information is incomplete as it does not take into account the cumulative damage to the structure. Experimental investigations have demonstrated that structural damage is a function of both peak as well as cumulative values. Normalised hysteretic energy (NHE) provides a good indication of cumulative damage in steel structures, and the results of those investigations by the authors are forthcoming.

REFERENCES

Barroso, L.R. (1999), *Performance Evaluation of Vibration Controlled Steel Moment Frames under Seismic Excitations*, Ph.D. Thesis, Dept. Civil & Environmental Engineering, Stanford University, California.

Barroso, L.R., S.E. Breneman and H.A. Smith (1998), "Evaluating the Effectiveness of Structural Control within the Context of Performance-Based Engineering". *Proc. of the 6th U.S. National Conference on Earthquake Engineering*, Seattle, Washington

Breneman, S.E. (1999), *Practical Design Issues in the Design of Active Control for Civil Engineering Structures*, Ph.D. Thesis, Dept. Civil & Environmental Engineering, Stanford University, California.

BSSC (1997), "NEHRP Guidelines for the Seismic Regulation of Exhisting Buildings and Other Structures," *Technical Report FEMA 273*, Building Seismic Safety Council, U.S.A.

Constantinou, M C, A. Mokha, and A. M. Rheinhorn (1991). "Study of Sliding Bearing and Helical-Steel-Spring Isolation System." *Journal of Structural Engineering,* 117(4), pp. 1257-1275.

Fu, Y. and K. Kasai (1998), "Comparative Study of Frames Using Viscoelastic and Viscous Dampers." *Journal of Structural Engineering,* 124(5), pp. 513-522.

Krawinkler, H.K. and A. Gupta (1998), "Story Drift Demands for Steel Moment Frame Structures in Different Seismic Regions." *Proc. of the 6th U.S. National Conference on Earthquake Engineering*, Seattle, Washington.

Somerville, P., D. Anderson, J. Sun, S. Punyamurthula, and N. Smith (1998), " Generation of Ground Motion Time Histories for Performance-Based Seismic Engineering*," Proc. 6th U.S. National Conference in Earthquake Engineering*, Seattle, Washington.

Wen, Y.K. (1976), "Method for Random Vibration of Hysteretic Systems." *Journal of the Engineering Mechanics Division*, 102(EM2), pp. 249-263.
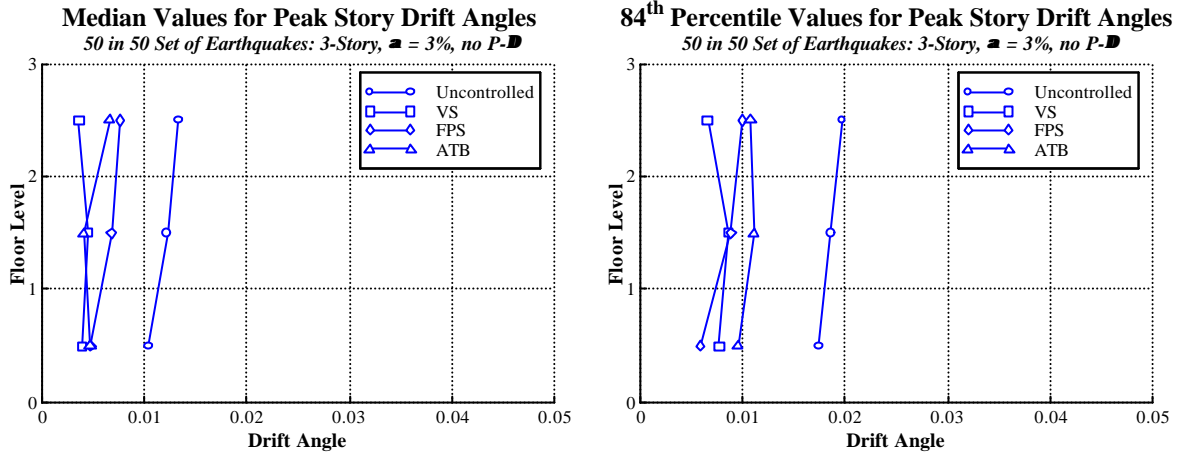
Figure 2: Statistical Story Drift Values under 50 in 50 Set of Ground Motions
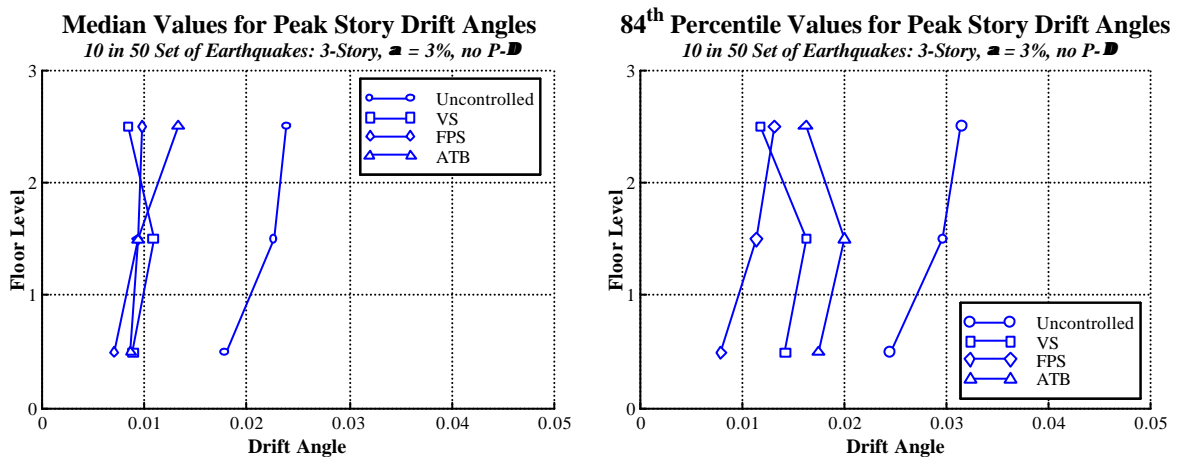
Figure 3: Statistical Story Drift Values under 10 in 50 Set of Ground Motions
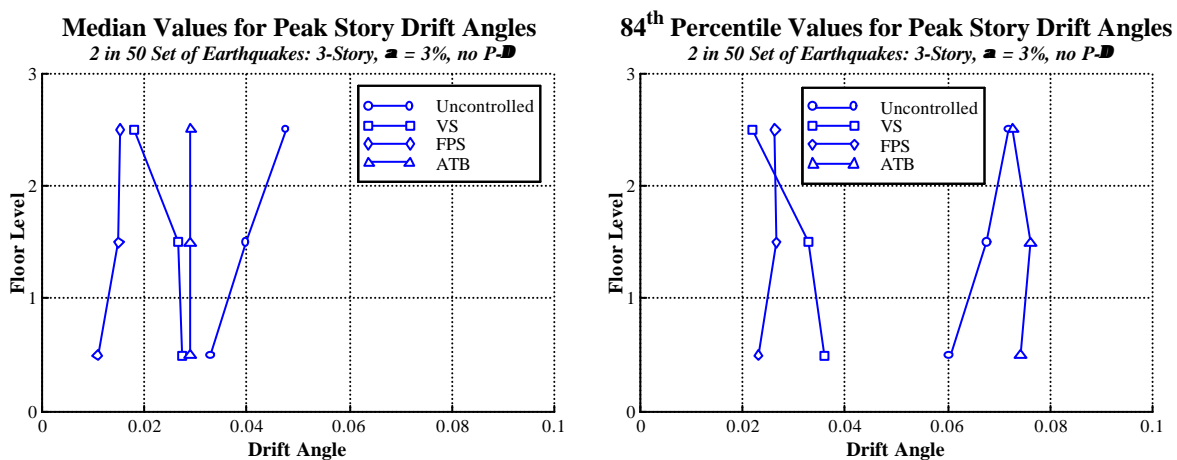
Figure 4: Statistical Story Drift Values under 2 in 50 Set of Ground Motions